HHS Public Access

Author manuscript

J Magn Reson Imaging. Author manuscript; available in PMC 2018 September 01.

Published in final edited form as:

J Magn Reson Imaging. 2017 September ; 46(3): 751–757. doi:10.1002/jmri.25611.

Whole-brain vessel wall MRI: A parameter tune-up solution to improve the scan efficiency of 3D variable-flip-angle turbo spin-echo

Qi Yang, MD, PhD[1,2,†], **Zixin Deng, MSc**[2,3,†], **Xiaoming Bi, PhD**[4], **Shlee S. Song, MD**[5], **Konrad H. Schlick, MD**[5], **Nestor R. Gonzalez, MD**[6], **Debiao Li, PhD**[2,3], and **Zhaoyang Fan, PhD**[2,*]

[1]Department of Radiology, Xuanwu Hospital, Beijing, China.

[2]Biomedical Imaging Research Institute, Department of Biomedical Sciences, Cedars-Sinai Medical Center, Los Angeles, CA, USA.

[3]Department of Bioengineering, University of California, Los Angeles, CA, USA.

[4]MR R&D, Siemens Healthcare, Los Angeles, CA, USA.

[5]Department of Neurology, Cedars-Sinai Medical Center, Los Angeles, CA, USA.

[6]Department of Neurosurgery, Cedars-Sinai Medical Center, Los Angeles, CA, USA.

Abstract

Purpose—To propose and evaluate a parameter tune-up solution to expedite a three-dimensional (3D) variable-flip-angle turbo spin-echo (TSE) sequence for whole-brain intracranial vessel wall (IVW) imaging.

Materials and Methods—Elliptical k-space sampling and prolonged echo train length (ETL), were used to expedite a 3D variable-flip-angle TSE-based sequence. To compensate for the potential loss in vessel wall signal, optimal combination of prescribed T_2 and ETL was experimentally investigated on 22 healthy volunteers at 3T. The optimized protocol (7–8 minutes) was then compared with a previous protocol (reference protocol, 11–12 minutes) in terms of signal-to-noise ratio (SNR), contrast-to-noise ratio (CNR), vessel wall sharpness, and wall delineation quality on a 4-point scale (0:poor; 3:excellent) in 10 healthy volunteers. A pilot study of 5 patients was performed and lesion delineation score was used to demonstrate the diagnostic quality.

Results—A protocol with ETL=52 and prescribed T_2=170ms was deemed an optimized one, which, compared to the reference protocol, provided significantly improved wall SNR (12.0±1.3 vs. 10.0±1.1, p=0.002), wall-lumen CNR (9.7±1.2 vs. 8.0±0.9, p=0.002), wall-CSF CNR (2.8±1.0 vs. 1.7±1.0, p=0.026), similar vessel wall sharpness at both inner (1.59±0.18 vs 1.58±0.14, p=0.87) and outer (1.71±0.25 vs. 1.83±0.30, p=0.18) boundaries, and comparable vessel wall

[*]**Corresponding Author:** Zhaoyang Fan, PhD, Biomedical Imaging Research Institute, Department of Biomedical Sciences, Cedars-Sinai Medical Center, 8700 Beverly Blvd., PACT 800, Los Angeles, CA 90048, Telephone: 310-248-8661, fanzhaoyang@gmail.com.
[†]These authors contributed equally to this work.

delineation score for individual segments (1.95–3, p>0.06). In all patients, atherosclerotic plaques (10) or wall dissection (5) were identified with a delineation score of 3 or 2.

Conclusion—A parameter tune-up solution can accelerate 3D variable-flip-angle TSE acquisitions, particularly allowed for expedited whole-brain IVW imaging with preserved wall delineation quality.

Keywords

Intracranial vessel wall; vessel wall imaging; 3D TSE; whole brain; magnetic resonance imaging

INTRODUCTION

Cerebrovascular disease, a major cause of morbidity and mortality worldwide, can arise from diverse intracranial vessel wall pathologies such as atherosclerosis, dissection, and vasculitis (1). Methods traditionally used for the diagnosis of cerebrovascular disease are based on lumenography imaging limited to the detection of luminal abnormalities, thus inadequate for differentiating various wall pathologies (2,3). Recently, there is a growing interest in high-resolution black-blood (BB) MRI due to its capacity to directly assess the intracranial vessel wall (IVW) and to potentially unravel etiology (4–7).

Three-dimensional (3D) turbo spin-echo (TSE) with variable refocusing flip angles has emerged as a promising BB MRI method for IVW imaging (8–12). Compared with previously used two-dimensional (2D) TSE methods, previous methods are more suited for small-sized, tortuous, and deep-seated intracranial arteries due to its 3D acquisition with flexible image reformatting and intrinsic advantages in resolution, signal-to-noise ratio (SNR), and spatial coverage. In most of previous studies (8–10,12) however, due to prohibitively long scan times, spatial coverage was often compromised where a thin imaging volume was used to achieve acceptable SNR and half-millimeter resolution while keeping a scan time of 6–8 minutes. As a result, lesions at distal branches might be missed.

Recently, inversion-recovery (IR) prepared SPACE (Sampling Perfection with Application-optimized Contrast using different flip angle Evolutions), IR-SPACE, was proposed as a 3D TSE approach, providing remarkable suppression of cerebrospinal fluid (CSF) signals, enhanced T_1 contrast weighting, and most importantly, whole-brain spatial coverage (13). Nevertheless, the technique still requires a scan time of over 11 minutes, potentially impeding its wide clinical application.

Further improvement in the scan efficiency of 3D variable-flip-angle TSE is clinically warranted. Typically, several imaging parameters in an MRI sequence can be tuned up for a balance between image quality and scan efficiency. Previous studies (8–10) commonly focused on echo train length (ETL) and repetition time (TR) to ensure acceptable SNR and/or desired contrast weighting, leaving little room for minimizing scan time. A few more imaging parameters, such as the T_1 and T_2 relaxation times used for calculating the refocusing flip angle series (14–16), are unique but have not been explored in terms of their potential of being utilized to reduce the scan time.

The present work aims at expediting a widely available 3D variable-flip-angle TSE-based sequence for IVW imaging, with a particular focus on the recently proposed IR-SPACE whole-brain imaging technique.

METHODS

The study was approved by the local institutional review board with written informed consent obtained from all subjects. A total of 22 healthy subjects and 5 patients with stroke or transient ischemic attack and suspected to have intracranial vasculopathies were recruited. Imaging was performed on a 3.0-T MRI system (MAGNETOM Verio; Siemens, Erlangen, Germany) equipped with a 32-channel head coil (Siemens, Erlangen, Germany).

Considerations in Improving Scan Efficiency

The original implementation of IR-SPACE for whole-brain IVW imaging employed 3D rectilinear sampling in both phase-encoding and partition-encoding directions, parallel imaging in the phase-encoding direction, and an intermediate ETL, resulting in a scan time of 11–12 minutes (13). To further expedite its data acquisition or a 3D variable-flip-angle TSE acquisition in general, elliptical k-space sampling and prolonged ETL are two straightforward strategies. Elliptical sampling in the k_y-k_z plane is known to accelerate scanning, despite slight drop-off in SNR and loss in high-frequency k-space information (17). This strategy along with radial reordering has been successfully applied to IVW MRI (8). Prolonged ETL, likewise, accelerates data acquisition but could be detrimental to SNR due to T_2-decay. However, SNR is intimately related to the applied refocusing flip angles that are calculated prospectively in order to achieve a desired, typically a certain steady-state, signal evolution given a set of imaging parameters including ETL, echo spacing, T_1, and T_2 (14–16). Hence, manipulation of T_1 and T_2 (denoted as prescribed T_1 and T_2) will directly affect refocusing flip angles and may be utilized to effectively compensate for the SNR loss caused by prolonged ETL.

Experimental Optimization

Imaging Experiments—To achieve sufficient SNR, the optimal combination of prescribed T_1/T_2 and ETL was experimentally investigated in the following steps.

I) To explore the effect of prescribed T_1 and T_2 on SNR and contrast-to-noise ratio (CNR): The commercial SPACE sequence based on which IR-SPACE was developed is, by default, for brain imaging and prescribed T_1/T_2 were set for gray matter, i.e. 940/100ms at 1.5-T (16). This setting may be suboptimal for IVW imaging at 3.0-T as the T_1/T_2 of both gray matter (1331/110ms, (16)) and arterial vessel wall (1114/55ms, (18)) are different from the pre-set values. Our preliminary testing (Supplementary Figure) in healthy subjects demonstrated that: 1) overall image SNR is affected more evidently by prescribed T_2 than by prescribed T_1; 2) setting prescribed T_1/T_2 based on the real relaxation times of the vessel wall poses degraded quality of IVW. We therefore focused on investigating the effect of prescribed T_2 while keeping prescribed T_1 fixed at 1100ms (i.e. the T_1 of the arterial vessel wall). Specifically, all prescribed T_2 values (50, 80, 110, 140, 170, and 200 ms) were tested in each of the 8 healthy subjects. The effect of prescribed T_2 was quantified by measuring

wall SNR, wall-lumen CNR, wall-CSF CNR, and white matter (WM)-gray matter (GM) CNR (indicative of the T_1 contrast weighting). To confirm whether the observed effect is independent of ETL, two different ETLs (36 and 60) were randomly selected in the 8 studies. Other common imaging parameters were listed in the Supplementary Table 1.

II) To confirm whether the effects of prolonged ETL on SNR and CNR is independent of prescribed T_2: For TSE sequences, empirically, a longer ETL lowers image SNR. Whether this trend is independent of prescribed T_2 was explored in 4 healthy subjects. Briefly, a range of ETLs, i.e. 36, 44, 52, 60, and 68, were respectively employed with prescribed T_2 fixed at 80ms or 170ms. The same quantitative metrics as mentioned above were determined.

Note, in step I and II, a commercial SPACE sequence was used where a non-selective saturation pulse along with a fixed saturation recovery time (620ms) was applied at the beginning of each TR and a minimal TR was used. This ensured the obtained SNR and CNRs were not confounded by different sequence timings associated with various parameter settings.

III) To identify an appropriate combination of ETL and prescribed T_2: Based on the findings from step I and II, a set of expedited IR-SPACE imaging protocols utilizing different prescribed T_2s (140, 170, or 200ms) with ETL=52, prescribed T_1=1100ms, elliptical sampling with radial reordering, and an adjusted TR from 800ms (as used in (13)) to 900ms to boost SNR, were compared with the reference protocol (i.e. ETL=36, prescribed T_1/T_2=940/100ms, rectilinear sampling, and TR = 800ms) in 10 additional healthy volunteers. In addition to SNR and CNR quantifications as mentioned above, the sharpness at the inner and outer vessel wall boundaries were also measured in this group. This latter metric was believed to exhibit an opposite trend to SNR and/or CNR as prescribed T_2 progressively deviates from the true T_2 (55ms) of the vessel wall (19). The protocol with the best trade-off between SNR/CNR and vessel wall sharpness was deemed as the optimized IR-SPACE protocol. The detailed imaging parameters were summarized in the Supplementary Table 1.

Image Analysis—The aforementioned SNR and CNRs were measured from the internal carotid artery supraclinoid segment (ICA C4) and its neighboring regions. On an image workstation (Syngo MultiModality Workplace; Siemens Healthcare, Germany), 2D cross-sectional images of 0.53-mm thickness were first reconstructed from individual 3D image sets for both the left and right ICA C4. Care was taken to ensure location match between different scans. On these 2D images, mean signal intensity (S) was then measured from the vessel wall of ICA C4, adjacent vessel lumen, CSF, WM, and GM using a region-of-interest (ROI) approach, and the noise, σ, was measured as the signal standard deviation from the sphenoid sinus cavity (artifact-free air region, ROI area > 200 mm^2) near the selected ICA C4 segments. From each scan, S of individual tissues was measured twice on the left and right sides, respectively, and averaged before calculating SNR (S/σ) and CNR ($[S_1-S_2]/\sigma$).

Vessel wall sharpness was also measured from the ICA C4 inner and outer wall boundaries. Using a previous method (20), sharpness was obtained at three dispersed locations of each vessel cross-section, and averaged among the locations of the left and right sides.

Statistical tests were performed in Step III only because of a relatively large sample size. SPSS (v.14.0, SPSS Inc., Chicago, IL, USA) was used with statistical significance defined as $p < 0.05$. A paired two-tailed Student's t test was used for the comparison of SNR, CNR and sharpness between each of the proposed expedited protocols and reference protocol.

Preliminary Evaluation of the Optimized IR-SPACE Protocol

The optimized protocol determined above underwent preliminary evaluation of image quality in both healthy and patients. In the 10 healthy subjects recruited during optimization step III, in addition to signal analysis described above, vessel wall delineation was further graded visually by two independent blinded readers (with 10 and 8 years of experience in MR vessel wall imaging) at the distal basilar artery (BA), the ICA C4, the middle cerebral artery (MCA) M1-M3 segments, the anterior cerebral artery (ACA) A1 and proximal A2 segments, and the posterior cerebral artery (PCA) P1 and proximal P2 segments from an arbitrarily selected side. The scores are given to reconstructed cross-sectional images based on a 4-point scale (0: ≤ 50% of the vessel wall is visible; 1: > 50% of the vessel wall is visible; 2: the vessel wall is delineated with adequate signal and contrast to the lumen and CSF; and 3: the vessel wall is delineated with excellent signal-to-noise ratio and sharp contrast to the lumen and CSF). The average score over the two readers was analyzed using a paired two-tailed Wilcoxon signed rank test for any difference between the optimized and reference protocols.

Additionally, the optimized IVW imaging protocol was assessed at pre- and post-contrast states in 5 patients. In 3 of them, the reference protocol was also performed before contrast injection for direct comparison with the optimized protocol. Due to contrast wash-out over time, comparison between reference and optimized protocols after contrast injection was not performed to avoid bias. All IVW image sets were rated by a neuroradiologist blinded to imaging protocols for the delineation quality of vessel wall lesions using a 4-point scale (0: poor; 3: excellent).

RESULTS

MR images were successfully acquired in all 22 healthy subjects (11 females, mean age 38 years). Progressively increasing prescribed T_2 from 50 up to 140ms could boost wall SNR, CSF SNR, wall-lumen CNR, wall-CSF CNR, and WM-GM CNR, when ETL was 36 (Fig. 1a) or 60 (Fig. 1b). This trend slowed down when T_2 reached 170ms. As expected, wall SNR, CSF SNR, and wall-lumen CNR decreased as ETL progressively increased from 36 up to 68, whereas wall-CSF CNR and WM-GM CNR were not markedly affected; these effects were observed at both a short (Fig. 1c) and long prescribed T_2 (Fig. 1d). Given the opposite effects from the two parameters, we simplified the optimization process by fixing ETL to 52, which permits a scan time of 7–8 min, and attempting to identify the best prescribed T_2 from a narrowed range, i.e. 140, 170, and 200ms.

The three expedited IR-SPACE imaging protocols all provided higher wall SNR, CSF SNR, wall-lumen CNR, wall-CSF CNR, and WM-GM CNR than the reference protocol did, as illustrated in Fig. 2a. Except for CSF SNR, significance in improvement was reached at a prescribed T_2 of 170 (12.0±1.3 vs. 10.0±1.1, p=0.002; 9.7±1.2 vs. 8.0±0.9, p=0.002; 2.8±1.0 vs. 1.7±1.0, p=0.026; 5.8±1.4 vs. 4.5±0.9, p=0.004 respectively) or 200ms (p=0.001, 0.001, 0.002, and 0.002, respectively). A higher prescribed T_2 generally led to higher wall SNR and CNRs. On the other hand, the three protocols generally led to similar or lightly lower (p>0.09 in all) vessel wall sharpness (e.g. for prescribed T_2 of 170: inner boundary 1.59±0.18 vs 1.58±0.14, p=0.87; outer boundary 1.71±0.25 vs. 1.83±0.30, p=0.18) (Fig. 2b). There was a trend that a higher prescribed T_2 resulted in a lower sharpness at the outer wall boundary. Thus, as a trade-off between SNR/CNR and wall sharpness, the combination of ETL of 52 and prescribed T_2 of 170ms was chosen as the optimized imaging protocol.

Despite the above differences between the optimized and reference protocols, they provided comparable vessel wall delineation quality for individual segments, as demonstrated in Fig. 3 and summarized in Supplementary Table 2.

Imaging was successfully performed in all 5 patients (2 females, age 41–64). Wall lesion delineation scores on pre- and post-contrast optimized VWI images were the same, i.e. 3 in 4 patients and 2 in 1 patient. The delineation quality of vessel wall lesions on the optimized IVW images was scored 3 in 4 patients and 2 in 1 patient. A total of 15 lesions were identified in 5 patients. Three cases (10 lesions) showed a focal lesion with eccentric wall thickening and contrast enhancement at the MCA, indicating intracranial atherosclerosis. Two case showed hyper-intense intramural hematoma at the internal carotid artery or vertebral artery, indicating dissection. Example images were shown in Fig. 4. There was no difference in score (all scored 3) between the optimized and reference protocols in the 3 patients who had both protocols performed, as illustrated in Fig. 5.

DISCUSSION

IVW MRI based on 3D variable-flip-angle TSE has demonstrated clinical promises in recent studies. The high demands for spatial resolution, SNR, and spatial coverage can pose prohibitively long scan times and hinder a wide adoption of this method. The present work proposed a parameter tune-up solution to accelerate the 3D acquisition while preserving image SNR and CNR. The solution was integrated into IR-SPACE based whole-brain IVW imaging and demonstrated reduction of scan time by over 30%, improvement in image SNR/CNR, and non-significantly impaired vessel wall sharpness as compared to the original IR-SPACE protocol. A 7-minute IVW scan using the optimized protocol could potentially improve subject tolerance and examination success rate.

Prescribed T_1 and T_2, as important parameters in the 3D variable-flip-angle TSE sequence, were commonly employed with vendor pre-set values. Theoretically, the real relaxation times of the vessel wall should be used in IVW imaging to calculate the flip angles that would give rise to a pseudo steady-state wall signal evolution and thus a potentially sharp wall delineation (17). This strategy has proven useful in a recent SPACE-based IVW imaging study at 7.0-T (19). However, at 3.0-T, poor wall SNR appears to markedly impair

IVW visualization (shown in Supplementary Figure), which could be exacerbated when elliptical sampling and prolonged ETL are both used to shorten scan time. We therefore focused the present work on enhancing SNR by identifying the optimized prescribed T_1 and T_2.

In this work, we demonstrated the effectiveness of prescribed T_2 in modulating overall image SNR. Within the interrogated range of prescribed T_2, a higher value generally led to higher wall SNR and CNRs of interest. However, since a prescribed T_2 that differs from true vessel wall T_2 can disturb the pseudo-steady state of the vessel wall and thus potentially cause vessel wall blurring, a trade-off between SNR/CNR and wall sharpness was necessary to determine the optimized prescribed T_2. This consideration is expected to be applicable for any application based on a 3D variable-flip-angle TSE sequence, although the optimal combination of prescribed T_2, ETL, and TR would be application dependent. Additionally, although demonstrated in a sequence with a variable radial k-space sampling pattern, the concept of using prescribed T_2 to modulate overall image SNR in 3D TSE imaging should hold true for other trajectories as this parameter is intimately related to flip angle series and resultant signal evolution.

The optimized protocol yielded significantly improved wall SNR and wall-CSF CNR while maintaining the desired T_1 contrast weighting, compared to the reference protocol. The SNRs of the vessel wall and CSF showed similar trend as prescribed T_2 or ETL changes. While the finalized optimal combination of prescribed T_2 and ETL favors the SNR of both the vessel wall and CSF, the benefit on the former outweighed that on the latter, leading to a significantly increased wall-CSF CNR. This is of importance for wall visualization given that poor contrast between the vessel wall and CSF has been one of major obstacles in intracranial vessel wall imaging. In addition, the overall WM-GM CNR, indicative of T_1 contrast weighting, was not only preserved but also significantly increased in the optimized protocol compared to the reference protocol. Thus, the optimized protocol is likewise highly suited for the detection of T_1-mediated high signal wall abnormality caused by intraplaque hemorrhage or lipid substances.

Vessel wall sharpness was not significantly reduced when using the optimized IR-SPACE protocol. Wall blurring can result from the prolonged, disturbed pseudo-steady state of the wall signal evolution and the elliptical sampling trajectory. However, these effects may be negligible compared to that of vessel pulsation-induced motion (21). Furthermore, the optimized protocol employs elliptical sampling in a radial fashion that is expected to maximally preserve the T_1 contrast weighting (22). Therefore, the contrast between vessel wall and its surrounding CSF at the ICA C4 can be enhanced, which may positively contribute to vessel wall sharpness.

There are some limitations in the study. First, computer simulations, typically useful for parameter optimization, were not performed. The k-space trajectory employed in commercial 3D variable-flip-angle TSE sequences is now implemented as a variable radial pattern (17,22). Varying ETL and prescribed T_2 will change both reordering scheme and signal evolution. Such variable signal distribution in k-space makes the quantification of signal intensity and sharpness of the vessel wall inaccurate when using computer simulation.

Second, in the pilot patient study, direct comparison between the optimized and reference protocols were conducted in 3 subjects only due to time constraints in the clinic. However, the good to excellent lesion delineation scores were obtained from all 5 cases. Third, the shortened scan time may also be traded for higher spatial resolution to provide more detailed assessment of small lesions, but, due to the limited sample size, this was not investigated in this work.

In conclusion, a parameter tune-up solution can accelerate the 3D variable-flip-angle TSE acquisitions, particularly allowed for expedited whole-brain IVW imaging with preserved wall delineation quality. Its potential in facilitating assessment of various cerebrovascular disease and wider clinical adoption of IVW MRI will require large-scale patient studies.

Supplementary Material

Refer to Web version on PubMed Central for supplementary material.

Acknowledgments

Grant Support: This work was supported in part by American Heart Association (15SDG25710441), National Institutes of Health (NHLBI 2R01HL096119), National Science Foundation of China (No.81325007, No. 81322022), and Program for New Century Excellent Talents in University (No.13-0918).

REFERENCE

1. Writing Group M. Mozaffarian D, Benjamin EJ, et al. Heart Disease and Stroke Statistics-2016 Update: A Report From the American Heart Association. Circulation. 2016; 133(4):e38–e360. [PubMed: 26673558]
2. Alexander MD, Yuan C, Rutman A, et al. High-resolution intracranial vessel wall imaging: imaging beyond the lumen. Journal of Neurology, Neurosurgery & Psychiatry. 2016; 87(6):589–597.
3. Bodle JD, Feldmann E, Swartz RH, Rumboldt Z, Brown T, Turan TN. High-Resolution Magnetic Resonance Imaging An Emerging Tool for Evaluating Intracranial Arterial Disease. Stroke. 2013; 44(1):287–292. [PubMed: 23204050]
4. Klein IF, Lavallee PC, Touboul PJ, Schouman-Claeys E, Amarenco P. In vivo middle cerebral artery plaque imaging by high-resolution MRI. Neurology. 2006; 67(2)
5. Niizuma K, Shimizu H, Takada S, Tominaga T. Middle cerebral artery plaque imaging using 3-Tesla high-resolution MRI. Journal of Clinical Neuroscience. 2008; 15(10):1137–1141. [PubMed: 18703337]
6. Swartz RH, Bhuta SS, Farb RI, et al. Intracranial arterial wall imaging using high-resolution 3-tesla contrast-enhanced MRI. Neurology. 2009; 72(7):627–634. [PubMed: 19221296]
7. Xu W-HH, Li M-LL, Gao S, et al. In vivo high-resolution MR imaging of symptomatic and asymptomatic middle cerebral artery atherosclerotic stenosis. Atherosclerosis. 2010; 212(2):507–511. [PubMed: 20638663]
8. Qiao Y, Steinman DA, Qin Q, et al. Intracranial arterial wall imaging using three-dimensional high isotropic resolution black blood MRI at 3.0 Tesla. Journal of Magnetic Resonance Imaging. 2011; 34(1):22–30. [PubMed: 21698704]
9. Natori T, Sasaki M, Miyoshi M, et al. Evaluating middle cerebral artery atherosclerotic lesions in acute ischemic stroke using magnetic resonance T1-weighted 3-dimensional vessel wall imaging. Journal of stroke and cerebrovascular diseases : the official journal of National Stroke Association. 2014; 23(4):706–711. [PubMed: 23871728]
10. Sakurai K, Miura T, Sagisaka T, et al. Evaluation of luminal and vessel wall abnormalities in subacute and other stages of intracranial vertebrobasilar artery dissections using the volume

isotropic turbo-spin-echo acquisition (VISTA) sequence: a preliminary study. Journal of neuroradiology Journal de neuroradiologie. 2013; 40(1):19–28. [PubMed: 22633047]

11. van der Kolk AG, Hendrikse J, Brundel M, et al. Multi-sequence whole-brain intracranial vessel wall imaging at 7.0 tesla. Eur Radiol. 2013; 23(11):2996–3004. [PubMed: 23736375]
12. van der Kolk AG, Zwanenburg JJ, Brundel M, et al. Intracranial vessel wall imaging at 7.0-T MRI. Stroke. 2011; 42(9):2478–2484. [PubMed: 21757674]
13. Fan Z, Yang Q, Deng Z, et al. Whole-brain intracranial vessel wall imaging at 3 Tesla using cerebrospinal fluid-attenuated T1-weighted 3D turbo spin echo. Magnetic resonance in medicine. 2016 PMID: 26923198.
14. Busse RF, Hariharan H, Vu A, Brittain JH. Fast spin echo sequences with very long echo trains: Design of variable refocusing flip angle schedules and generation of clinical T2 contrast. Magnetic Resonance in Medicine. 2006; 55(5):1030–1037. [PubMed: 16598719]
15. Mugler JP, Bao S, Mulkern RV, et al. Optimized single-slab three-dimensional spin-echo MR imaging of the brain. Radiology. 2000; 216(3):891–899. [PubMed: 10966728]
16. Park J, Mugler JP, Horger W, Kiefer B. Optimized T1-weighted contrast for single-slab 3D turbo spin-echo imaging with long echo trains: application to whole-brain imaging. Magnetic resonance in medicine. 2007; 58(5):982–992. [PubMed: 17969106]
17. Busse RF, Brau A, Vu A, et al. Effects of refocusing flip angle modulation and view ordering in 3D fast spin echo. Magnetic Resonance in Medicine. 2008; 60(3):640–649. [PubMed: 18727082]
18. Wang J, Helle M, Zhou Z, Börnert P, Hatsukami TS, Yuan C. Joint blood and cerebrospinal fluid suppression for intracranial vessel wall MRI. Magnetic Resonance in Medicine. 2016; 75(2):831–838. [PubMed: 25772551]
19. Viessmann O, Li L, Benjamin P, Jezzard P. T2-Weighted intracranial vessel wall imaging at 7 Tesla using a DANTE-prepared variable flip angle turbo spin echo readout (DANTE-SPACE). Magnetic Resonance in Medicine. 2016 PMID: 26890988.
20. Li D, Carr JC, Shea SM, et al. Coronary arteries: magnetization-prepared contrast-enhanced three-dimensional volume-targeted breath-hold MR angiography. Radiology. 2001; 219(1):270–277. [PubMed: 11274569]
21. Nishida T, Kinoshita M, Tanaka H, Fujinaka T, Yoshimine T. Quantification of Cerebral Artery Motion during the Cardiac Cycle. American Journal of Neuroradiology. 2011; 32(11)
22. Mugler JP 3rd. Optimized three-dimensional fast-spin-echo MRI. J Magn Reson Imaging. 2014; 39(4):745–767. [PubMed: 24399498]

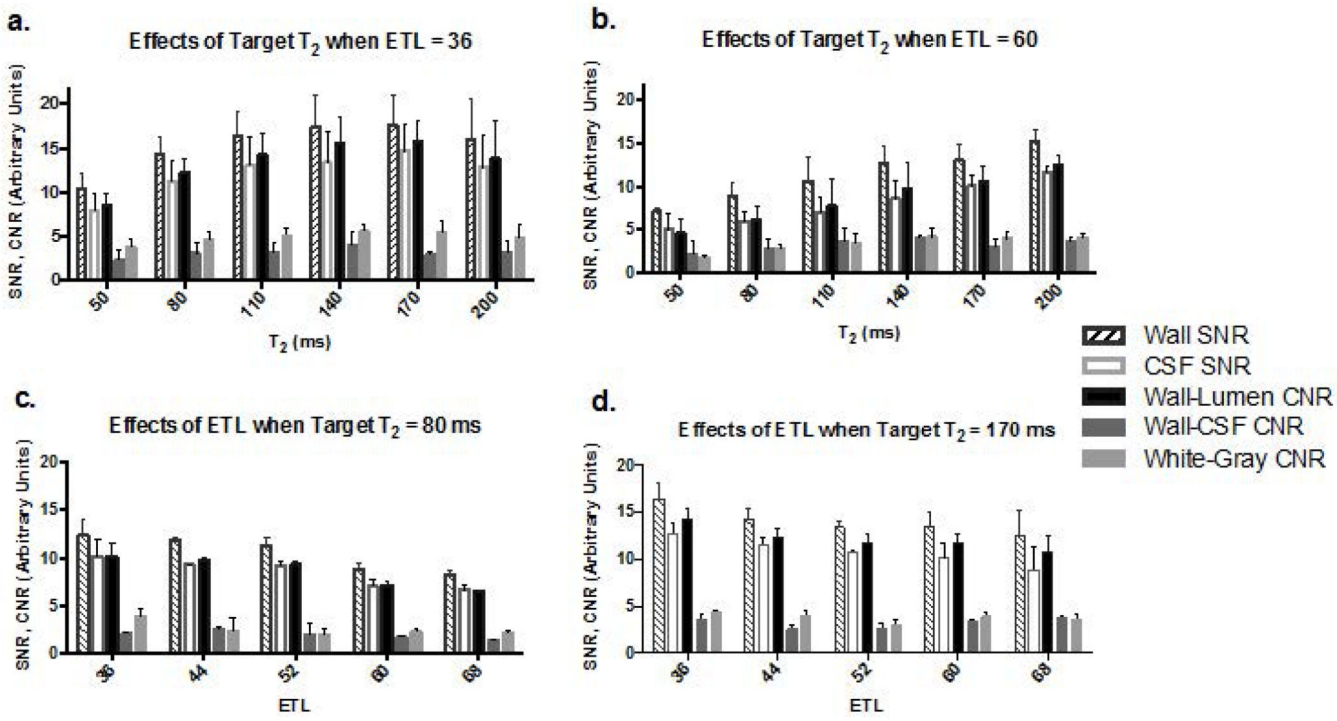

Figure 1.

Effects of prescribed T_2 (a & b.) and echo train length (ETL) (c & d.) on wall signal-to-noise ratio (SNR), CSF SNR, wall-lumen contrast-to-noise ratio (CNR), wall-CSF CNR, and white-gray matter CNR in selected scenarios.

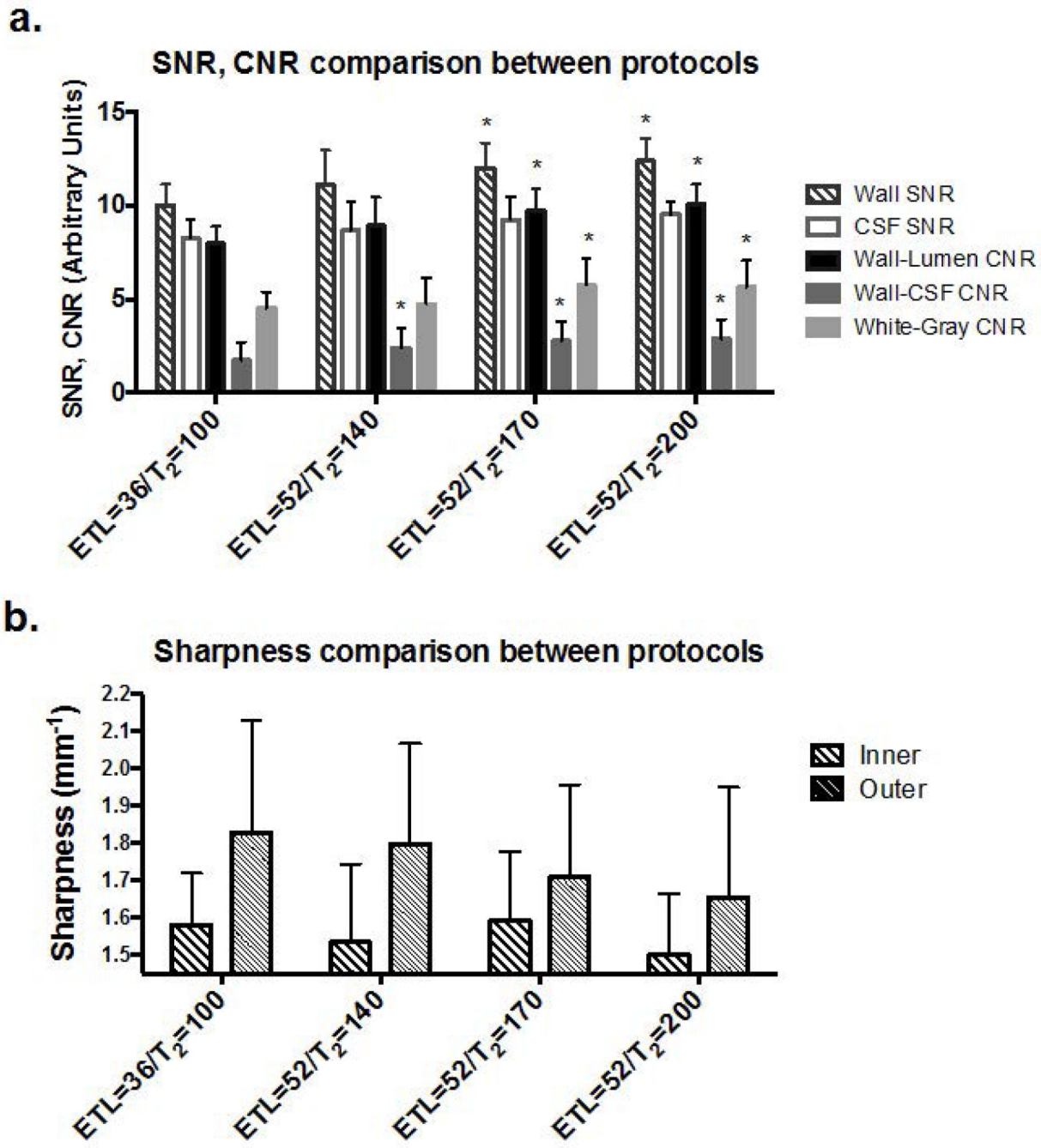

Figure 2.

Comparison of three expedited whole-brain IR-SPACE protocols (echo train length [ETL] = 52) to the reference protocol (i.e. previously proposed long-duration protocol whereby ETL = 36). For SNR/CNR comparisons (a), the expedited protocol with a prescribed T_2 of 170 or 200 ms provided significant (marked with *) improvements. For wall sharpness comparisons (b), a general trend of decrease in vessel wall sharpness was observed as prescribed T_2 increased, especially at the outer wall boundary. However, deterioration was not statistically significant with any of the expedited protocols.

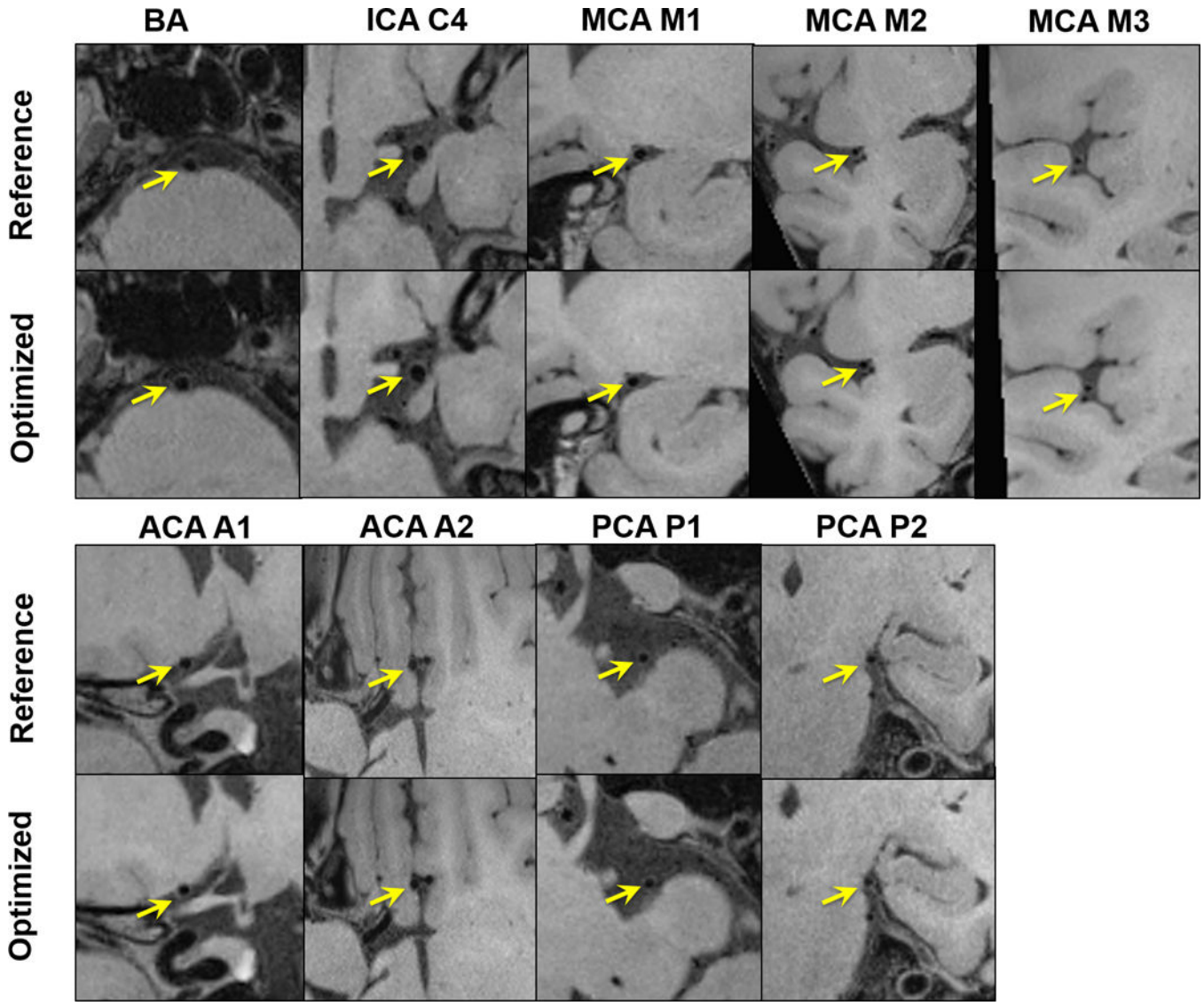

Figure 3.

Comparison between the reference protocol (i.e. previously proposed protocol whereby echo train length [ETL] = 36, prescribed T_2 = 100 ms) and the optimized protocol (i.e. ETL = 52, prescribed T_2 = 170ms) in one healthy volunteer. Example images of the basilar (BA), internal carotid artery (ICA) C4, middle cerebral artery (MCA) at M1, M2, M3 segments, anterior cerebral artery (ACA) at A1, proximal A2 segments, and posterior cerebral artery (PCA) at P1, proximal P2 segments. Comparable image quality is observed between the two imaging protocols.

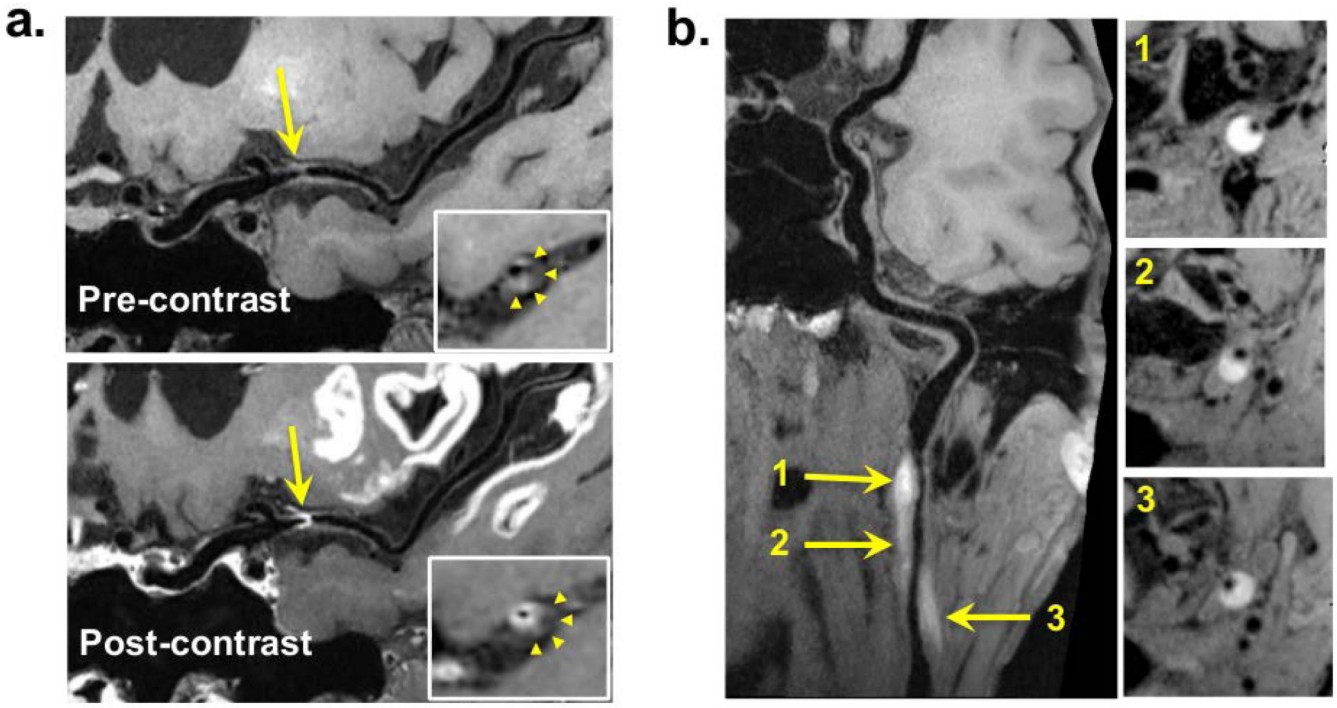

Figure 4.

Example patient images with curved multi-planar reconstruction. a) In a 58-year-old male patient, intracranial vessel wall (IVW) imaging reveals a focal lesion at the left middle cerebral artery M1 segment. It is characterized by eccentric wall thickening (arrows), suggestive of a plaque, on pre-contrast images and strong enhancement (arrows) at the plaque-lumen interface instead of in the entire thickened wall (arrowheads in the zoomed-in cross-sectional images) on post-contrast images. b) In a 51-year-old male patient, dissection at the left internal carotid artery, IVW imaging reveals a lesion (arrows) at the left internal carotid artery with hyper-intense, crescent-shaped intramural hematoma and longitudinally diffuse involvement.

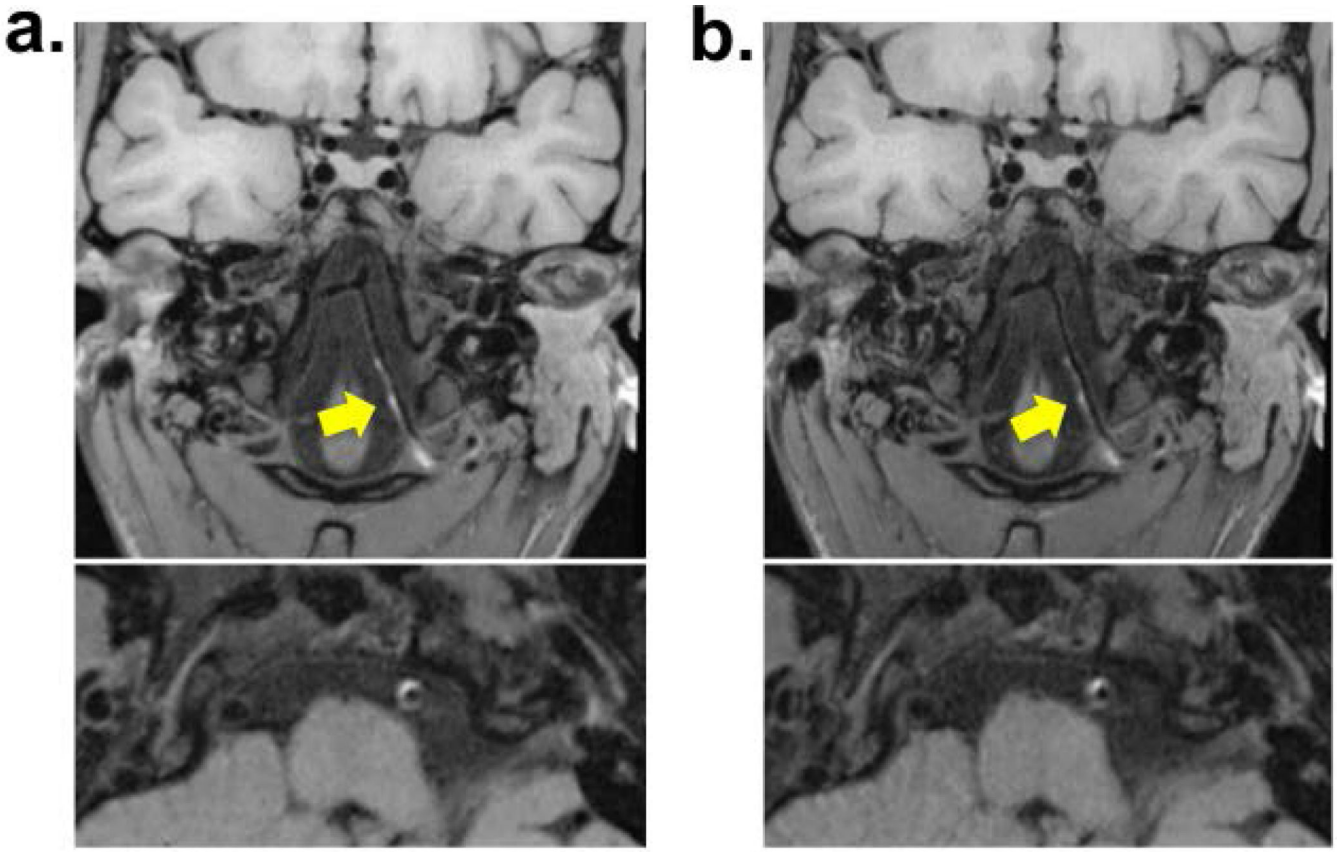

Figure 5.

Comparison between the optimized protocol (a) and the reference protocol (b) in a 28-year-old female patient with dissection at the left vertebral artery. Longitudinally diffuse hyperintense intramural hematoma was depicted comparably by both protocols.